

Development of the Brain Tissue Scanner  
Brain Networks Laboratory Technical Report

## Development of the Brain Tissue Scanner

Bruce H. McCormick  
Brain Networks Laboratory  
Department of Computer Science  
Texas A&M University  
College Station, TX, USA  
mccormick@cs.tamu.edu

Last Updated: March 18, 2002

## Table of Contents

### **1. Overview of the Instrument**

- 1.1 Configuration of the instrument
  - Precision positioning system and ultramicrotome
  - Image capture system
  - Image analysis and data storage system
- 1.2 Acquisition of volume data
- 1.3 Current instrument status and support software
  - Precision positioning system and ultramicrotome
  - Image capture system
  - Image analysis and data storage system
  - 3D reconstruction
  - Database support for 3D reconstruction and modeling
- 1.4 3D reconstruction experiments

### **2. Tissue Block Specifications**

- 2.1 Dimensions of the rodent brain
  - Adult mouse data source
  - Adult rat data source
  - Shrinkage upon embedding
- 2.2 Mounts for whole rodent brain
  - Design problem
  - Proposed solution
  - Rodent brain blocking tools
  - Recommended mold sizes
- 2.3 Mounts for human cortical tissue
  - From gross anatomy to microstructure
  - Mosaic blocks of human cortical tissue
- 2.4 Tissue blocks scheduled for sectioning and scanning

### **3. Precision Positioning System and Ultramicrotome Specifications**

- 3.1 Performance requirement: aligned image stack/volume data set
- 3.2 System components
- 3.3 Work piece and its physical sectioning
- 3.4 Stage 3D coordinate system: home positions and directions of travel
  - Home positions and directions of travel
  - World coordinates for the work piece
- 3.5 Three-axis stage performance specifications
  - X-axis linear air-bearing stage
  - Y-axis positioning stage
  - Z-axis compact vertical lift stage
  - Three-axis motion controller
  - Stage base and custom bridge
  - Filtered air utility
- 3.6 Diamond knife specifications for ultramicrotomy
  - Knives for 3D microstructure reconstruction
  - Wide knife for rodent brain surveys and building 3D brain atlases
  - Diamond knife durability

### 3.7 Specimen carrier specifications

- Water system for the specimen carrier
- Specimen module
- Waterproof laser-knife connector
- Diamond knife holder accommodations for underwater microtomy

## **4. Image Capture System Specifications**

### 4.1 Performance requirement: mouse brain scanned a high resolution in under 1 month

### 4.2 Line-scan camera specifications

- Camera specifications
- Time delay integration (TDI)
- Binning

### 4.3 Microscope objectives specifications

- Resolving power of an objective
- Number of resolvable pixels
- Water-immersible objectives
- Imaging with the Nikon CFI 60 Fluor water-immersible series of objectives
- Comparison with prototype tissue imaging
- Imaging with the low-power Nikon CFI 60 dry objectives

### 4.4 Illumination system specifications

- Illumination requirements at sensor
- Illumination requirements at the source
- Laser line generators: line width selection

### 4.5 Microscope assembly

- Microscope objective focusing and retracting system
- Camera transfer lenses

### 4.6 Camera interface cards for image acquisition

### 4.7 Camera test configuration for the CT-F3 camera

- 50mm macro lens
- Other Schneider Optics components

## **5. Image Analysis and Data Storage System Specifications**

### 5.1 Performance requirement: Real-time image data compression and 1TB dynamic data storage

### 5.2 Image analysis and data storage system configuration

- Multi-server storage system
- Gigabit switching network

## **6. Brain Tissue Scanning**

### 6.1 Brain tissue scanning modes

- Monochrome high-resolution mode (neurons and fibers)
- Color high-resolution mode (neurons and fibers)
- Monochrome low-resolution mode (cell counts and somata morphology)
- Color low-resolution mode (cell counts and somata morphology)

### 6.2 Data volumes for the rodent brain

- Block dimensions (plastic-embedded brain)
- Data volumes/sweep (mouse brain, worst case)
- Data volumes/sweep (rat brain, worst case)
- Total data volumes (mouse brain, no compression)
- Total data volumes (rat brain, no compression)

### 6.3 Rodent brain scanning times

Development of the Brain Tissue Scanner  
Brain Networks Laboratory Technical Report

**7. Acknowledgments**

**8. References**

## List of Tables

- Table 1. Rodent brain weights and dimensions
- Table 2. Specification for the line-scan cameras
- Table 3. Nikon CFI 60 Fluor Water-Immersion Objectives (coherent illumination)
- Table 4. Low-power Nikon CFI 60 Fluor Dry Objectives (coherent illumination)
- Table 5. CWS power requirements at the sensor
- Table 6. Fractions of scattered and fluorescence illumination captured by the objective
- Table 7. Transmission factors for optical train
- Table 8. Illumination requirements at the source
- Table 9. Illuminated line aperture at tissue surface
- Table 10. Data volumes/sweep (mouse brain, worst case)
- Table 11. Data volumes/sweep (rat brain, worst case)
- Table 12. Total data volumes (mouse brain, no compression)
- Table 13. Total data volumes (rat brain, no compression)
- Table 14. Mouse scanning times (unburdened by overhead)
- Table 15. Rat scanning times (unburdened by overhead)

## List of Figures

- Figure 1. Schematic of precision positioning system, showing granite base and bridge (Aerotech, Inc.).
- Figure 2. Specimen undergoing simultaneous sectioning and line scanning. Nikon CFI 60 Fluor 40X NA 0.8 objective is on left, diamond knife on right. Specimen carrier shown schematically.
- Figure 3. Reconstruction viewed from top of slab. Neurons are represented by their central trajectories. (Vertical axis stretched). [4]
- Figure 4. Neuronal iso-surfaces for a subset of the previous data as computed from the marching cubes algorithm [4].
- Figure 5. Stage coordinates (a right-handed coordinate system)
- Figure 6. Work piece coordinate (a right-handed coordinate system)
- Figure 7. Fraunhofer diffraction at a circular aperture [Born and Wolfe, 9]

# Development of the Brain Tissue Scanner

## 1. Overview of the Instrument

A new instrument of our design, the *Brain Tissue Scanner* [8,9], will allow the reconstruction of mammalian brain architecture. The instrument has been designed to volume digitize at 200MHz a specimen (e.g., a plastic-embedded tissue block) at 250nm sampling resolution. The instrument delivers an aligned three-dimensional mesh of uniform volume elements (voxels): Voxels are assigned digital signal amplitudes for each optical channel (wavelength) used in scanning the specimen. Physical sectioning is used to circumvent photon-limited image capture (a speed requirement). No deconvolution of the imagery is necessary. The speed of the instrument is such that we anticipate an entire mouse brain (~1cm<sup>3</sup>) can be scanned in one month (one-shift operation).

### 1.1 Configuration of the instrument

The instrument hardware is composed of three major subsystems described below.

#### Precision positioning system and ultramicrotome

(Aerotech Inc., Pittsburgh, PA; Micro Star Technologies, Huntsville, TX). The specimen block is mounted atop a three-axis precision stage (Figure 1). The custom diamond knife, rigidly mounted over the stage, cuts from the block consecutive serial thin sections. Under numerical control the stage and knife together perform as an ultramicrotome, cutting sections typically 0.5µm thick. The sectioning process destroys the tissue block. Following current practice in semiconductor inspection instrumentation, direct-drive and linear encoders are used in the 3-axis stage. The precision positioning system uses an air-bearing stage for the X-axis (cutting axis), and encoder resolutions of 20nm for the X- and Y-axes and 25nm for the vertical Z-axis. These tolerances insure that images from consecutive serial sections are automatically registered into an aligned image stack, or volume data set.

#### Image capture system

(Dalsa, Canada; EPIX, Inc., Buffalo Grove, IL; Micro Star Technologies, Huntsville, TX). Either of two high-sensitivity line-scan cameras (Dalsa CT-F3-4096 pixels, monochrome, or Dalsa CL-T5-2048 pixels, color) images the newly-cut thin section just beyond the knife edge, prior to subsequent deformation of the tissue (Figure 2). The microscope objective, aligned perpendicular to the top surface of the diamond knife (and hence at 45° to the vertical), images the knife-edge. The tissue is imaged using either of two recently introduced Nikon CF160 water immersion objectives: the CFI Fluor 10X (NA 0.3) and the CFI Fluor 40X (NA 0.8). These objectives have two advantages: Their 45° access angle allows them to fit within the fold between the uncut and newly cut tissue, and being water-immersion, these objectives have higher numerical aperture, and hence resolution. These objectives are mounted in a truncated Nikon Eclipse E600FN microscope (designed for electrophysiology using patch clamp technology). A choice of diode laser line generators (green: 532nm, 50mW or blue: 473nm, 30mW; StockerYale, Canada) illuminate tissue at the diamond knife tip with a 30-100µm wide strip of intense illumination. The diamond knife serves dual use: (1) as an optical element (prism serving as the microscope collimator) and (2) for physical sectioning. The intensity of the knife-edge illumination allows line sampling at 44kHz (for the Dalsa CT-F3 camera) and 10.7kHz (for the Dalsa CL-T5 color camera). Alignment of the laser line-generator, diamond knife, microscope optical train, and line-scan camera is established by a custom collimating assembly (Micro Star Technologies, Huntsville, TX).

Two objectives of lower power (Nikon CF160 2X and 4X) are also provided for gross anatomy studies and for 3D brain atlas construction. Both objectives are used dry, without water immersion.

Image acquisition passes the digital video signal from the camera to the first of multiple servers of the image capture system. Uninterrupted video transmission is demanded during the pass of the knife

Development of the Brain Tissue Scanner  
Brain Networks Laboratory Technical Report

across the specimen block. A gigabit fiber network links the servers, such that subsequent image analysis can be distributed over all servers.

### Image analysis and data storage system

To recognize regions of interest (ROIs) in serial sections in real time, and thereby achieve a 50-fold data reduction for Golgi-stained tissue (or an estimated 16-fold reduction for GFP-stained tissue), the brain tissue scanner is being equipped with a cluster of 5 servers. Each server is equipped with 1.0GHz Pentium 3 dual processors (three with 1.3GHz dual processors) and 2 GB SDRAM memory. The system provides 1.04TB of SCSI hard drive storage (typically 5 drives/server, each 36GB or 72GB). Each server is also provided with a gigabit fiber server adapter to configure the network using a conventional Cisco gigabit network switch. The operating system of the server cluster was Windows 2000 Server, in conformity with available camera interface card drivers, but is being replaced by Linux.

### 1.2 Acquisition of volume data

*Knife-edge scanning*<sup>1</sup> not only preserves image registration throughout the depth of the specimen block but also optically isolates the tissue above the knife from that below to eliminate undesirable events (back-scattering of light and bleaching of fluorescent-stained tissue below the knife). Knife-edge scanning supports all known forms of microscopy (absorption imaging using transmitted light; reflected light imaging using bright-field, dark-field, and DIC; and fluorescence imaging).

Consider the acquisition of volume data from a mouse brain embedded in a plastic block (13mm A-P x 9.5mm M-L x 6mm D-V). A 40X objective has a *field of view* (knife width) of 0.625mm. Sixteen strips (each 0.625mm wide by 13mm long) are cut for each Z-axis section (like plowing a field). For a block height of 6mm, 12,000 sections must be cut, each 0.5 $\mu$ m thick. The integrated tissue ribbon length (13mm/strip x 16 strips/section x 12,000 sections) is 2.5km.

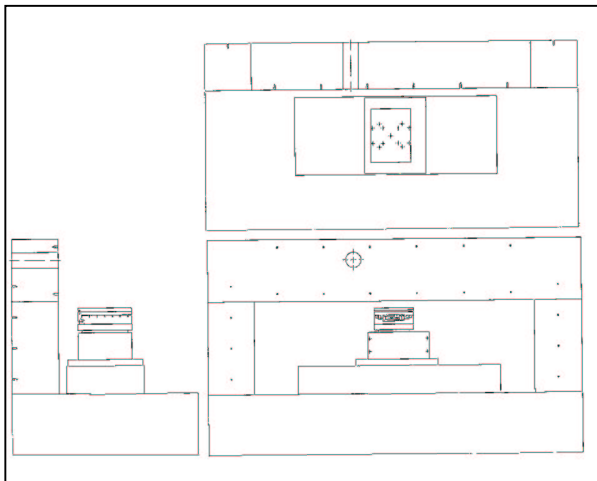


Figure 1. Schematic of precision positioning system, showing granite base and bridge (Aerotech, Inc.).

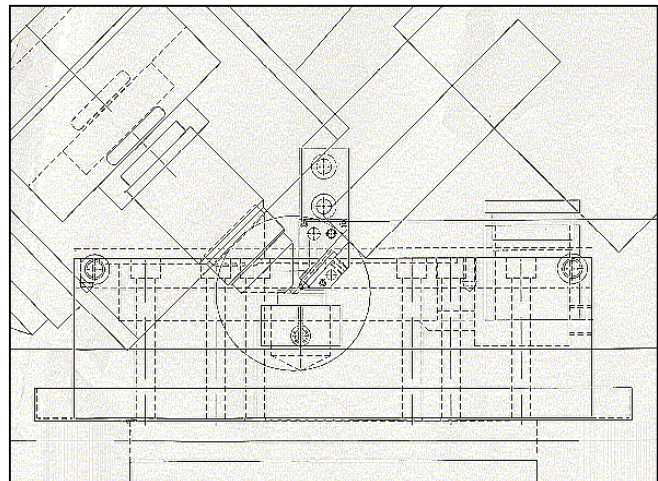


Figure 2. Specimen undergoing simultaneous sectioning and line scanning. Nikon CF1 60 Fluor 40X NA 0.8 objective is on left, diamond knife on right. Specimen carrier shown schematically.

The tissue ribbon will be line-sampled  $10^{10}$  times at 250nm resolution, corresponding to the Nyquist sampling interval for an ideal optical resolution of  $0.77 (532\text{nm})/0.80 \text{ N.A.} = 512 \text{ nm}$ . The tissue ribbon

<sup>1</sup> A patent application, "System and Method for Imaging an Object", covering all aspects of knife-edge scanning, has been submitted by the Texas Engineering Experiment Station (TEES, McCormick, 1451) to the U. S. PTO on September 6, 2001.

## Development of the Brain Tissue Scanner Brain Networks Laboratory Technical Report

can be scanned at 11mm/s by line sampling at 44kHz, the camera maximum. The 2.5km tissue ribbon requires 227,000s = 63hr. There are obvious inefficiencies because mice brains are not cubical, stage return times, etc., so we fold-in 60% overhead, to attain an estimated 100hr. This time per mouse brain is well within one month, our target time. Image acquisition is presently limited by the data acquisition rate of available cameras.

### **1.3 Current instrument status and support software**

#### Precision positioning system and ultramicrotome

The Aerotech precision positioning system has been installed. The air micro-filtration system (XXX) for the air-bearing stage has also been installed. The stage is currently being programmed for the required knife-edge scanning choreography. The diamond knife of the ultramicrotome, embedded as the collimator assembly (described above), will be rigidly mounted to the massive granite bridge overhanging the three-axis stage.

#### Image capture system

The Dalsa CT-F3 line-scan camera, frame buffers/camera controllers, and initial dual-processor server passed acceptance tests at the vendor before shipment. A Dalsa CL-T5 color line-scan camera, until recently removed by Dalsa for redesign, has been ordered with delivery expected in January 2002. All other parts (Nikon Eclipse 600FN microscope body, CF160 objectives, diode-laser line generators) of the system are in-house and are being designed into a collimator assembly by Micro Star Technologies. The system, complete with custom diamond knives, should be operational by Spring 2002.

#### Image analysis and data storage system

The initial configuration of 5 servers and Cisco gigabit switch is operational. The Linux cluster operating system, replacing Windows 2000, is being installed. .

#### 3D reconstruction

The reconstruction process comprises four stages [3,4]. First, each sectional image is independently segmented into regions of interest (ROIs), and encapsulated in oriented bounding boxes. The image-based segmentation, running in real time, reduces ~50-fold (for Golgi-stained tissue) the requirements for secondary storage, as is critical in a production environment potentially generating over one teravoxel per day. Second, ROIs from successive images are threaded together into cell trajectories. Pathway branching and merging and bends are accommodated at this stage. Third, identified cell segments are edited into viable dendritic or axonal arbors, or somata, using stochastic models of the neurons/forests. Selective visualization of the reconstructed cells is provided. Finally, inter-neuronal connectivity is estimated using probabilistic roadmap methods (PRMs).

#### Database support for 3D reconstruction and modeling

McCormick and Koh [5-7] describe a distributed database system supporting 3D reconstruction and modeling. The database exoskeleton is isolated from inevitable changes in reconstruction and modeling software.

### **1.4 3D reconstruction experiments**

In pilot parallel reconstruction experiments described in [4], Golgi-stained cortical material was sectioned at 0.5 $\mu$ m increments using an ultramicrotome equipped with a diamond knife designed for histological sectioning. Forty-two consecutive sections were digitized at 1024 x 1024 pixels at a linear resolution of 370nm and then digitally aligned into a coherent volume data set. Our reconstruction program, Recon [3,4], determined regions of interest (ROIs) in each image and culled data aggressively,

reducing the original volumetric data 70-fold into a ROI-based aligned image stack. The neuronal forest of Figures 3 and 4 below were threaded from this reduced data set.

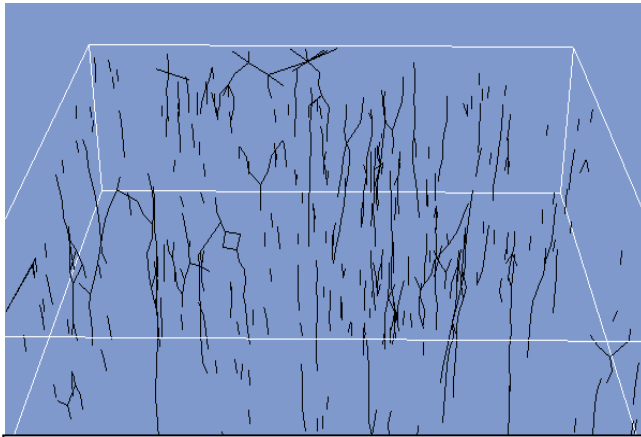


Figure 3. Reconstruction viewed from top of slab. Neurons are represented by their central trajectories. (Vertical axis stretched). [4]

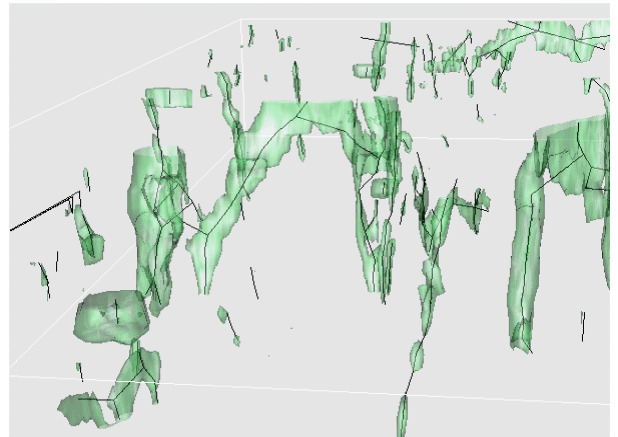


Figure 4. Neuronal iso-surfaces for a subset of the previous data as computed from the marching cubes algorithm [4].

## 2. Tissue Block Specifications

### 2.1 Dimensions of the rodent brain

Specimen mounts in design are compatible with cutting blocks of entire rodent brain: mouse or rat in sagittal or coronal orientation. For the rat when cut in coronal orientation, its A-P length (22mm) unfortunately extends beyond the maximum allowable depth of cut, namely the 12.5mm travel of the Z-axis stage. At present we have no resolution of this issue other than cutting the brain into two pieces. But such cuts require major software surgery to sew together the fine fibers crossing the cut, and the cutting process distorts the tissue. For the mouse, cutting in any of the three orientations is possible. However mounts will be provided only for sagittal and coronal orientations; the expense of additional design for the third orientation was unwarranted.

Unlike human brain, rodent brains continue to grow throughout life so there is no fixed size. Also, we will be cutting brains of both younger and older animals. Given the vagaries of these sizes, several molds will be made for both mouse and rat. (James Fallon, UCI, provided the data in Table 15 and recommendations below.)

Table 1. Rodent brain weights and dimensions

Rodent	Brain weight (g)	A-P length (mm)	M-L width (mm)	D-V height (mm)
mouse	26-30	13	9.5	6
rat	270-310	22	15	10

#### Adult mouse data source

Franklin and Paxinos, *The Mouse Brain in Stereotaxic Coordinates*, Academic Press, 1997. Study used 26 fully adult male C57BL/J6 mice, 77-78d old 26-30g. Mice strains show more variance in brain and body size and anatomy than rats, but this atlas is just right for our adult male studies.

### Adult rat data source

Paxinos and Watson, *The Rat Brain in Stereotaxic Coordinates*, Academic Press, 1986 and later. Study used 130 male Wistar rats, 270-310g (average = 290g). Rats' bodies and brains keep growing until they die. A fully mature rat will weigh 436g and a juvenile weighs 180g. A 150g young juvenile will produce a brain 2 mm smaller than the 290g atlas value. This is a 10% reduction.

### Shrinkage upon embedding

The above mouse/rat dimensions were derived from 4% paraformaldehyde fixed, frozen sections, embedded in gelatin. Using paraffin or plastic, there will be shrinkage. Actual sizes are 5-8% smaller than the figures above. Therefore the dimensions given are upper limits.

## **2.2 Mounts for whole rodent brain**

### Design problem

Consider a plastic cylinder 25mm in diameter and 18.5mm long. The rodent brain (or semi-brain for the rat brain when cut in coronal section) must be embedded in top 12.5mm of this plastic cylinder in the proper orientation for either coronal or sagittal sectioning.

Why these constraints? The brain must be held absolutely rigidly in position, otherwise the knife will chatter while sectioning. The maximum travel of the Z-axis (elevator) stage is 12.5mm, and so only this depth can be cut. Furthermore the bottom 6mm of the cylinder is clamped and held with embedding plastic in a circular mount rigidly attached to the stage, with inner diameter 25mm and height 6mm.

### Proposed solution

Provide molds for casting each half of the above cylinder (split lengthwise), with hollows for the mouse (rat) brain held in proper orientation. The rodent is dipped in embedding compound, and clamped between the previously prepared left and right halves of the molded cylinder -- to make a plastic cylinder of the above dimensions. This scheme requires four molds for each rodent species and specimen size: one each for 2 orientations (coronal/sagittal) x 2 halves of the final cylinder (left and right halves). The molds will be cast using a solid model of the rodent brain, numerically machined from a solid model of the brain derived from the Paxinos et. al. 2D brain atlases (ibid.).

### Rodent brain blocking tools

A blocking tool is used to get the blocking angle identical to that used in the atlas (so we can match atlas pictures). For the mouse, we will use a D Kopf blocking tool, which also can be obtained from A. Peters, Science Tech Center, Carleton University, Ottawa, Ontario, Canada K1S 5B6 613-520-4442. The same source also provides a blocking tool for the rat.

### Recommended mold sizes

Three sizes will be made for both rat and mouse, with a full range of difference of 20% (+/- 5% higher and 15% lower than given above). In total, 24 molds are required: 2 species x 3 sizes per species x 2 orientations (coronal/sagittal) x 2 halves of the cylindrical mold.

## **2.3 Mounts for human cortical tissue**

### From gross anatomy to microstructure

[Koh and McCormick, 6] presents a way to preserve the coherence between thick sections (~1mm thick) of cortical tissue and 3D reconstructions of its microstructure. Here using longer strokes, typically 20-50mm, can reduce sectioning overhead.

## Mosaic blocks of human cortical tissue

As many as 20 pieces of tissue (ea. 4mm x 4mm x 3mm) can be molded into a mosaic specimen block with integrated tissue volume = 1 cm<sup>3</sup>. From the view of efficient use of the BTS, this is much preferable to sectioning individual pieces, which entails excessive repositioning of the stage. For human brain tissue, we plan to use a 3mm slab of embedded tissue containing a mosaic of 4 x 4 x 3 pieces.

### **2.4 Tissue blocks scheduled for sectioning and scanning**

We plan to proceed as follows with BTS testing:

1. **Sectioning tests:** (a) at 500nm thickness with 0.625mm effective knife width and (b) at 600nm and 1200nm thickness with 2.5mm effective knife width. (Note: Only half the diamond knife is used in cutting; the other half is held in reserve for when the first half-knife dulls. The physical knife widths used above are 1.25mm and 5mm respectively.) Cutting speeds of 1.5mm/s, 11mm/s; 44mm/s (for 2.5mm knife width only). These test the choice of embedding plastic and degradation of tissue at higher cutting speeds (if any). Blocks should approximate in size an embedded mouse brain.
2. **Absorption imaging tests** (initially at 532nm; monochrome imaging): with a variety of stains: Golgi, Nissl, whatever is important.
3. **GFP fluorescent imaging tests** (monochrome imaging; initially at 473nm. (Should GFP fluorescence in the 473nm band prove inadequate, we could turn to the 488nm band, which only became available from Coherent in May 2001.)
4. **XFP fluorescence tests** (color imaging; initially at 473nm). (Later tests will use the 488nm band, if that proves necessary.) These tests will use the color camera. Color cutting times are four times longer – a restriction of available line-scan color cameras.
5. **Everything else (fluoro-gold, DiI, etc.)** Order of preference, and whether to scan in monochrome or in color, has yet to be determined. Changing to another block within one of the tests, (1)-(5) above is essentially trivial from the perspective of the BTS. Also changing from the 40X objective to the 10X objective (as for cell counting) should prove minor. However the change between fluorescence and absorptive imaging may entail new technical problems, as the change from monochrome to color imaging certainly will.

The initial results will at best establish feasibility of knife-edge scanning. We do not expect to use the data for reporting neuroanatomical microstructure results. Before reporting neuroanatomical data, we propose to improve (1) the histological procedures (provided by UCI), (2) the knife-edge scanning techniques, and in particular (3) the 3D reconstruction and visualization software. At that time all data will be provided open source on Internet II.

## 3. Precision Positioning System and Ultramicrotome Specifications

### **3.1 Performance requirement: aligned image stack/volume data set**

Our objective is to scan repeatedly the topmost section of the work piece—the block of stained brain tissue embedded in plastic (Figure 1) – as consecutive thin sections are cut away by the sectioning diamond-knife, and new surfaces are exposed. Knife-edge scanning generates a *volume data set in the form of an aligned image stack*. The design of the brain tissue scanner (BTS) is predicated on maintaining vertical registration of consecutive surface scans. All sectioned material is destroyed.

### **3.2 System components**

The precision positioning system and ultramicrotome consists of three components:

1. The *precision positioning system* provides a platform that holds the tissue block and provides numerical control of the ultramicrotome.

2. The *ultramicrotome*, configured as a sledge microtome, uses a custom diamond knife for physical sectioning of tissue.
3. The *specimen carrier*, mounted atop the vertical (elevator) positioning stage, clamps the tissue specimen (work piece) and maintains its surface under 2mm of water, in conformity with the 2mm working distance of the water immersion objectives used in the instrument. For low-power 2X and 4X objectives,

### 3.3 Work piece and its physical sectioning

- Material: brain tissue embedded in plastic
- Bounding volume (max): tissue mounts restrict cuts to cylinder (25mm dia. x 12.5mm depth).
- Sectioning thickness (typically uniform for entire work piece): 0.25-10 $\mu$ m
- Section thickness indexed by vertical lift stage
- Vertical repeatability (1 count): 25nm

### 3.4 Stage 3D coordinate system: home positions and directions of travel

#### Home positions and directions of travel

The stage conventions for home positions and directions of travel are set at the time of manufacture by Aerotech, Inc. The conventions selected are:

X-axis stage: lower (X) axis homes to the left end of the stage and positive motion is to the right.

Y-axis stage: lower (Y) axis homes to the front and positive motion is toward the rear.

Z-axis stage: lower (Z) axis homes at the bottom and positive motion is upward.

#### World coordinates for the work piece

In the brain tissue scanner, the air-bearing stage with work piece moves left-to-right along the X-axis when knife-edge cutting/line-scanning.

We are using computer graphics conventions for world coordinates (Figure 6): the 3-dimensional work piece is viewed as if by a camera positioned above the workspace, looking downward along the stage Z-axis. The world coordinate system is right-handed and the object (work piece) is normally considered to reside in the negative-z half-space. We use x, y, and z for the coordinate of the volume data set generated by the knife-edge scanning.

X-axis: home is at work piece right, increasing to work piece left

Y-axis: home is at work piece rear, increasing toward the work piece front

Z-axis: home is at work piece top, increasing upward (work piece is in negative z half-space)

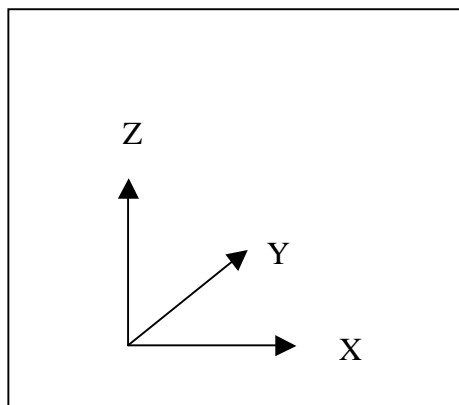


Figure 5. Stage coordinates (a right-handed coordinate system)

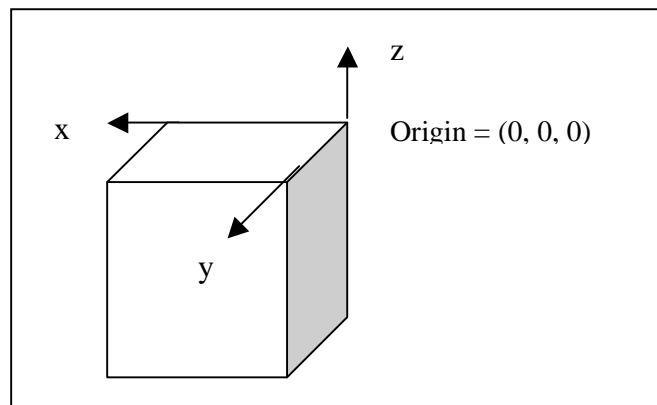


Figure 6. Work piece coordinate (a right-handed coordinate system)

Cutting/scanning conventions for mapping stage coordinates to world coordinates of the work piece are:

- X-axis scanning: increment X-axis position of stage. Map X-coordinate to x by translation
- Y-axis scanning: increment Y-axis position of stage. Map Y-coordinate to y by translation
- Z-axis scanning: increment Z-axis position of stage. Map Z-coordinate to z by inversion and translation.

### **3.5 Three-axis stage performance specifications**

#### **X-axis linear air-bearing stage**

An air-bearing stage is used to avoid knife clatter during microtomy.

Travel: 300mm

Accuracy in X direction: Limited importance

Accuracy in Z direction: Repeatable 300nm cuts

Cutting velocity: 1-50mm/s

Min. cycle time: 0.5s (25mm); 1s (max. travel)

Settling time: Not significant for line-scanning; stage used only for scanning and cutting

Linear resolution: 20nm

Repeatability (1 count): 20nm; maintains alignment of images in the image stack

Limit switches on home position and maximum travel

#### **Y-axis positioning stage**

Min. travel: 50mm

Min. travel speed: 4mm/s

Linear resolution: 20nm

Repeatability (1 count): 20nm

Stage settling time: <300ms

Limit switches on home position and maximum travel

#### **Z-axis compact vertical lift stage**

Uses wedge design for vertical lift to maximize resolution and stability

Min. travel: 12.5mm (maximum commercially available)

Max. travel speed: 3mm/s

Resolution: 25nm

Repeatability (1 count): 25nm

Stage settling time: < 300ms

Limit switches on home position and maximum travel

#### **Three-axis motion controller**

Three-axis bus-based motion control board

Driver chassis

Motion control PC

Man-machine interface (via U500 software)

#### **Stage base and custom bridge**

Granite base (48" x 24" x 8")

Custom bridge assembly (see Figure 1)

Custom welded steel stand, supports granite base

### Filtered air utility

Pressure/filtration system for air-bearing stage (also used with vertical lift stage):

Typical pressure should be maintained between 70-80psi. (80psi is recommended but should not be exceeded.)

Pressure regulation: 2%

Flow: 0.25-0.50 cfm

Dryness: -40 degrees F.

Filtration: fine

Supplier: Balston division, Parker Filtration Products

### **3.6 Diamond knife specifications for ultramicrotomy**

#### Knives for 3D microstructure reconstruction

Goal: To scan mounted brain tissue at 40X and 10X resolution, to permit detailed neuronal-level three-dimensional reconstruction of the tissue.

Knife material: Diamond

Knife widths: 1.25mm (with 40X objective) and 5mm wide (with 10X objective). Tissue cutting uses either the left or right half of the knife: 0.625mm (with the 40X objective) and 2.5mm (with the 10X objective).

Knife illumination types: At each width one knife will be designed for transmission illumination (absorption imaging) and one knife for epi-illumination (fluorescence imaging).

Thin section thickness: 0.25-2.0 $\mu$ m

Cutting speeds (plastic embedding/0.5 $\mu$ m): 1- 50mm/s

Diamond knife bracket with 3-axis adjustment

A zoom microscope with attached video camera is used to align diamond knife with laser line-generator, and microscope optical train

#### Wide Knife for rodent brain surveys and building 3D brain atlases

Goals: To scan whole rodent (mouse and rat) brain sections at 2X and 4X resolution. These resolutions would be used for rodent brain surveys and for building three-dimensional brain atlases, providing a sorely needed navigational tool within the rodent brain microstructure.

Knife material: Diamond

Knife width: 12.5mm. Tissue cutting uses either the left or right half of the knife with the 4X objective and full width of knife for 2X objective.

Knife types: One knife will be designed for transmission illumination (absorption imaging) and one knife for epi-illumination (fluorescence imaging).

Cutting speeds (plastic embedding/2.5-10 $\mu$ m): >1.5mm/s.

Diamond knife bracket with 3-axis adjustment

A zoom microscope with attached video camera is used to align diamond knife with laser line-generator, and microscope optical train.

#### Diamond knife durability

An additional issue concerns knife durability. Bernard Mesa, President, Micro Star Technologies, gives the example of Micro Star's machining of the copper disks upon which they polish diamond blanks to a sharpness of 5nm width at the knife tip. These copper disks have a diameter of 8", with a concentric hole of 4". The final surface trim cut is made with a diamond knife tool with a rounded diameter of 100 $\mu$ m. A copper ribbon of ~17 $\mu$ m width and 1 $\mu$ m thickness is cut. The lathe spindle velocity is 280rpm = 4.67 rev/s. From this data one can calculate two parameters of interest: the average cutting velocity (= 2,240mm/s) and the integrated length of the ribbon trailing out behind the knife (1.43km).

## Development of the Brain Tissue Scanner Brain Networks Laboratory Technical Report

We hypothesize that cutting hard plastic is no worse than cutting copper. This says first that one could cut the plastic at a speed of ~2,200mm/s, or 200 times the maximum cutting velocity we plan for high-resolution knife-edge scanning. This option is not available to us, as our maximum rate of cutting is limited by the maximum data rate of the Dalsa CT-F3 camera, the highest data rate camera commercially available, to 11mm/s when line sampling at 250nm.

Secondly, the diamond knife (which is sharpened for the final trim cut of each copper disk) has a useful life of ~1.43km, or 57% of the 2.5km (plastic, not copper) ribbon length for an entire mouse brain. However, copper is appreciatively more abrasive than plastic – it's for this reason that copper disks are used to polish diamond knives. And secondly, one diamond tool commonly can be used more than once for the final trim cutting of a copper polishing disk. Conclusion: One knife sharpening should suffice for cutting tissue at 0.5 $\mu$ m and scanning an entire mouse brain at 250nm X-Y resolution.

### **3.7 Specimen carrier specifications**

#### Specimen carrier

This unit bolts atop Z-axis lift stage and includes: (1) a precision locating receptacle for the specimen module (see below), (2) a water containment trough for immersed ultramicrotomy operation, (3) water level sensor, (4) water level adjustment, (5) splash lid, (6) splash tray, (7) water inlet and outlet. The inlet is coupled to the diamond knife holder and provides suctioning of the sections next to the diamond knife edge. The carrier is designed for a specimen cutting depth of 12.5mm.

#### Water system for the specimen carrier

This unit includes automatic level control, valves, pump, pump control, flow control, filter, and water reservoir. The level control works automatically to replenish water loss due to evaporation or splashing. To lower the water level a drain valve is manually operated. Normally system tries to maintain 2mm of filtered water above top surface of specimen

#### Specimen module

This is a simple and reproducible way of mounting and attaching specimens in the collimator assembly. Six molds and 18 specimen mounts will be supplied. The molds and specimen mounts are reusable. The sizes of the molds are discussed above in Section 2.2. The BTS is designed to run unsupervised and fully automated during microtomy operation. Hitting a hard surface during this cutting would ruin the diamond knife. Hence the molds add a shank to the bottom of the rodent brain by which the brain can be firmly held. Furthermore, these mounts are pin registered to the specimen carrier: Mounts can be removed and replaced without realignment.

#### Water-proof laser-knife connector

The laser line-generation lens will be inside the specimen carrier during ultramicrotomy operation. This connector prevents water from interfering with the optical path between the laser and the diamond knife.

#### Diamond knife holder accommodations for underwater microtomy

This holder includes a water inlet and water connection for suctioning the section during ultramicrotomy. It also includes a receptacle for attaching the waterproof laser-knife connector. Diamond knives will be supplied already mounted and precision positioned in their holders. Four holders are supplied with the system.

## 4. Image Capture System Specifications

### 4.1 Performance requirement: mouse brain scanned a high resolution in under 1 month

For a first orientation, consider a typical work piece: 13mm x 9.5mm x 6mm (741mm<sup>3</sup> = 0.741cm<sup>3</sup>). This block holds one mouse brain. For the human cerebral cortex, this volume approximates 15 cortical samples, each 4mm x 4mm x 3mm = 48mm<sup>3</sup>. A typical human brain developmental study entails 8 age points x 5 brains/age point x 50 cortical areas/brain = 96 cm<sup>3</sup> of tissue. As a rule of thumb, no federal agency supports (without Congressional authorization) experiments whose data acquisition runs  $\geq$  3-5 years. In this light the target scanning time of 1 cm<sup>3</sup>/month is critically important. We will see below that this criterion translates into an average image acquisition rate of 1.5TB/working day.

### 4.2 Line-scan camera specifications

#### Camera specifications

Two line-scan cameras, whose specifications are summarized in the Table 2 below, are used in the BTS.

Table 2. Specification for the line-scan cameras

Specification	Dalsa CT-F3 (monochrome)	Dalsa CL-T5 (color)
Resolution	4906 x 96 TDI	2048 x 24/24/48 TDI (R/G/B)
Pixel Size	13 $\mu$ m x 13 $\mu$ m	14 $\mu$ m x 14 $\mu$ m
Aperture	53.3 x 1.3mm	28.7 x 1.6mm
Lens Mount	Custom	F-mount
Max. Line Rate	44 kHz	10.7 kHz
Data Rate	8 x 25 MHz	3 x 25 MHz
Data Format	8x8-bit LVDS	3x8-bit LVDS
Responsivity	180 DN/(nJ/cm <sup>2</sup> )	380/260/220DN/(nJ/cm <sup>2</sup> ) (R/G/B)
Dynamic Range	610:1	R/G/B: 330/330/280:1
Nominal Gain Range	Fixed	6-17.5x

#### Time delay integration (TDI)

An external trigger generated by the PSO option of the stage controller drives either camera. Sampling increments are typically  $\geq$ 250nm, while the air-bearing stage has a resolution of 20nm, or a resolution advantage of 12.5:1. However, image blurring could arise from bunching of newly cut tissue within a 24 $\mu$ m (40X imaging) or 106 $\mu$ m (10X imaging) of the knife-edge, when using the maximum number of available TDI stages.

#### Binning

Binning is not available with these cameras, but can be emulated in real time by software.

### 4.3 Microscope objectives specifications

#### Resolving power of an objective

The *field of view (FoV)* of an objective is the diameter of the largest circular area in object space that can be simultaneously viewed with specified spatial integrity. The linear array of a line-scan camera sensor images a line in the object plane of this diameter. Microscope objectives are designed to fill the microscope tube (typically ~25mm). Accordingly the FoV is given by

$$FoV = \frac{\text{tube diameter}}{M} .$$

Development of the Brain Tissue Scanner  
Brain Networks Laboratory Technical Report

The minimum distance  $\Delta Y$  between two resolvable points in the object plane [Born and Wolf, 1] is given by

$$\Delta Y \approx 0.77 \frac{\lambda_0}{N.A.} \quad (\text{coherent illumination})$$

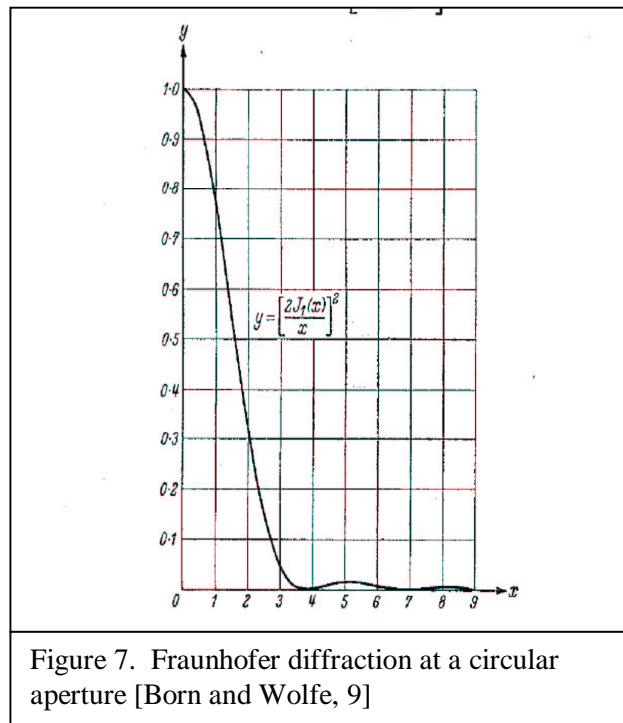
and

$$\Delta Y \approx 0.61 \frac{\lambda_0}{N.A.} \quad (\text{incoherent illumination})$$

where  $\lambda_0$  is the nominal wavelength of the illumination, and the numerical aperture, N.A., of the objective is given by

$$N.A. = n \sin \theta .$$

Here,  $n$  is the index of refraction of the object medium, and  $2\theta$ , the *angular aperture* on the object side, is the angle that the diameter of the entrance pupil of the objective subtends for the point centered in the objective's field of view. Figure 7 illustrates the Airy disk defined by diffraction induced by the entrance pupil of the objective [Born and Wolf, 2]. Here,  $\Delta Y$  is the radius of the central Airy disk. This theoretical criterion for maximum resolution neglects any further image degradation by the objective lens, the field lens of the microscope, and the transfer lens matching the output of the microscope field lens to the camera.



### Number of resolvable pixels

A minimum number of pixels in the linear array,  $N_{\min}$ , is required such that light from neighboring resolvable points in the object plane is focused upon adjacent pixels:

$$N_{\min} = \frac{FoV}{\Delta Y} .$$

For example, using green laser illumination ( $\lambda_0 = 532\text{nm}$ ) with a water-immersible Nikon CFI 60 Fluor 10X objective (N.A. = 0.3, tube diameter = 25mm, FoV = 2.5mm), we deduce

$$N_{\min} = \frac{2.5\text{mm}}{1.37\mu\text{m}} = 1825 \text{ pixels.}$$

To avoid aliasing, the Nyquist criterion asserts that we must use a linear array with  $2N_{\min} = 3,650$  pixels minimum—possible only with the CT-F3-4096 camera. This theoretical limit on resolution, while accommodating diffraction induced by the objective aperture, ignores image degradation by the subsequent lenses of the optical train.

### Water-immersible objectives

A limitation of knife-edge scanning has been finding objectives of sufficiently high numerical aperture (NA) that can focus the top edge of the knife and yet can be positioned within the fold between the uncut tissue block and the newly cut tissue, as it drapes over the knife. Every objective, being axially-symmetric, fits within a cone co-axial with its optical axis and extending from its center of focus. The minimum angle of this cone that contains the objective is known as its *access angle*. For use with a knife having an edge angle of  $45^\circ$ , this objective access angle must be  $\leq 45^\circ$ . This constraint is not necessarily met by objectives of long working distance. It is a different and the critical criterion for knife-edge scanning.

In a recent development, Nikon has introduced a line of high-performance water-immersible objectives for researchers employing electrophysiology and related applications. The objectives are ideal for capturing image data in physiology and live cell work. The objectives include the CFI Fluor 10X NA 0.3, CFI Fluor 40X NA 0.8, CFI Fluor Phase DLL 40X NA 0.8, and CFI Fluor 60X NA 1.0. All are designed for immersion into the perfusion media, offer a consistent 2mm working distance, and can be used for differential interference contrast, fluorescence and brightfield, giving optimal transmission over a broad spectrum of wavelengths. The objectives are part of Nikon's CFI60 series of infinity optics. The thermally and electronically insulated objectives have high transmission from the low ultraviolet range, ideal for FURA-2 work, all the way through to the near-infrared spectrum, for thick brain slice recordings. The 10X and 40X objectives have a narrow front that provide a  $45^\circ$ -access angle. All of the objectives in Nikon's physiology series offer the highest numerical apertures, making them the best available objectives for low light level fluorescence for applications requiring the highest resolution in optical physiology techniques.

Accordingly we have chosen to initially use the Nikon CFI Fluor 40X N.A. 0.8 and the CFI Fluor 10X N.A. 0.3 as the best available objectives for knife-edge scanning. Axons, mostly sub-micrometer in diameter, are at the ragged edge of optical detection. Here the 33% increase in optical resolution, obtained with water-immersible objectives, is critical. In reality, the 40X objective must be ground on one side of the objective lenses to provide specimen clearance. This operation is not guaranteed. Although Micro Star is confident that this can be done successfully, there is a possibility that one or both of the lenses be damaged, in which case Micro Star will not be responsible for replacing the lenses. (The Nikon CFI 60X N.A. 1.0 objective offers a  $35^\circ$  access angle, and can not be used in the present design, though the objective may be ground on one side so as to meet our required  $45^\circ$  access angle constraint.)

### Imaging with the Nikon CFI 60 Fluor water-immersible series of objectives

For the Nikon series below we identify 10X, 40X, and potentially 60X objectives. We tabulate in Table 3 the magnification (M), numerical aperture (N.A.), working distance (W.D.), and field of view (FoV) of the objective. For three wavelengths of light: blue (473nm), green (532nm), and red (670nm), we tabulate the resolving power (RP), defining the theoretical minimum resolvable distance between two points in the object plane and the number of resolvable pixels ( $N_{\min}(\lambda)$ ). Here  $\frac{1}{2}$  RP is the sampling interval specified by the Nyquist sampling theorem. The number of pixels in the linear sensor array should be  $2N_{\min}$ , to avoid aliasing of the image data.

Table 3. Nikon CFI 60 Fluor Water-Immersion Objectives (coherent illumination)

M	N.A.	W.D. (mm)	FoV (mm)	Blue (473nm)		Green (532nm)		Red (670nm)	
				½ RP (nm)	2 $N_{\min}$	½ RP (nm)	2 $N_{\min}$	½ RP (nm)	2 $N_{\min}$
10X	0.3	2	2.5	607	4,120	683	3,660	860	2,910
40X	0.8	2	0.625	228	2,750	256	2,440	322	1,940
60X	1.0	2	0.417	182	2,290	205	2,040	258	1,620

#### Comparison with prototype tissue imaging

A prototype image stack was built from digitized images (each 1024 x 1024 pixels) of serial 0.5 $\mu$ m sections using incoherent illumination [4]. The digitized images physically corresponded to a 370 $\mu$ m x 370 $\mu$ m square of tissue, as viewed by a 40X objective. The maximum field of view (FoV) for a 40X objective is 0.625mm. However, the effective FoV, as constrained the relay lens of the camera, is given by the diagonal of the imaged square, or  $\sqrt{2}(0.370)mm = 0.523mm$ , representing  $\frac{\sqrt{2}(0.370mm)}{0.625mm} = 84\%$  of the maximum FoV.

The resolving power (RP) of the 40X objective, interpolating from the Zeiss Epiplan-Neofluar objectives for green incoherent illumination, is given by 570nm. Nyquist sampling at ½ RP gives 285nm, rather than the 370 $\mu$ m/1024 = 361nm used. This would argue that the images were under-sampled by 27%.

The number of pixels in an equivalent line-scan camera would have been  $\sqrt{2}(1024) = 1,448$  pixels. Had Nyquist sampling been used, the linear array would have been 0.523mm/285nm = 1,835 pixels; and had the full FoV been used at this resolution, the linear array would have needed 1.27 x 1,835 = 2,331 pixels. By Table 3 above, the equivalent Nyquist sampling with the water-immersion Nikon 40X objective requires 2,440 pixels. The lower numerical aperture of the air objective is largely compensated by the lower resolution attainable using coherent (laser) illumination.

#### Imaging with the low-power Nikon CFI 60 dry objectives

Paralleling above, we tabulate for the Nikon CFI 60 dry Apo objectives the magnification (M), numerical aperture (N.A.), working distance (W.D.), and field of view (FoV) of the objective (Table 4). For three wavelengths of light: blue (473nm), green (532nm), and red (670nm), we tabulate the resolving power (RP), defining the theoretical minimum resolvable distance between two points in the object plane and the number of resolvable pixels ( $N_{\min}(\lambda)$ ). Here ½ RP is the sampling interval specified by the Nyquist sampling theorem. The number of pixels in the linear sensor array should be  $2 N_{\min}$ , to avoid aliasing of the image data.

Table 4. Low-power Nikon CFI 60 Fluor Dry Objectives (coherent illumination)

M	N.A.	W.D. (mm)	FoV (mm)	Blue (473nm)		Green (532nm)		Red (670nm)	
				½ RP (nm)	2 $N_{\min}$	½ RP (nm)	2 $N_{\min}$	½ RP (nm)	2 $N_{\min}$
2X Apo	0.1	8.5	12.5	1,820	6,870	2050	6,100	2,580	4,850
4X Apo	0.2	15.7	6.25	910	6,870	1025	6,100	1,290	4,850

### 4.4 Illumination system specifications

#### Illumination requirements at sensor

Table 5 gives the CWS power requirements at the sensor. For each camera we calculate the light flux (nJ/cm<sup>2</sup>) required for saturation (DN = 255), using all available TDI registers, then the aperture of the

sensor ( $\text{cm}^2$ ), and hence the total light energy per exposure (nJ). For each camera (and color) the CW illumination power is computed for knife-edge scanning at the maximum line rate allowed by the camera.

Table 5. CW power requirements at the sensor

Camera	Dalsa CT-F3-4096)	Dalsa CL-T5-2048 (color)		
		R	G	B
Saturation light flux ( $\text{nJ}/\text{cm}^2$ )	1.42	0.671	0.981	1.16
Aperture area ( $\text{cm}^2$ )	0.693	0.115	0.115	0.230
Saturation light exposure (nJ)	0.984	0.077	0.113	0.267
CW power ( $\mu\text{W}$ ) at maximum line rate	43.3	0.82	1.21	2.86

### Illumination requirements at the source

The BTS optical chain starts at the exit port of the laser line generator, passes through the diamond knife collimator, enters the microscope objective, passes through the filter cube and the field lens of the microscope, and finally enters the transfer lens matching the output of the field lens to the aperture of the line-scan camera. At each stage there are significant transmission losses, of which the greatest is dictated by the fraction of light captured by the entrance pupil of the objective. For fluorescence imaging, additional losses are entailed by the quantum efficiency of the fluorescence.

An estimate of the fraction of scattered (fluorescent) light,  $f_{scatt}$  ( $f_{fluor}$ ) captured by the objective can be made from  $2\theta$ , the *angular aperture* on the object side, defined as the angle which the diameter of the entrance pupil of the objective subtends for the point centered in the objective's field of view. The angular aperture can be calculated from the numerical aperture of the objective, using  $N.A. = n \sin \theta$ . For water-immersible objectives, the index of refraction, n, is  $n = 1.33$ . For absorptive imaging, a worst-case estimate assumes that the light is scattered uniform over the hemisphere centered over the scattering center. In this case we find  $f_{scatt} = (1 - \cos \theta)$ . For fluorescence imaging, a more accurate estimate can be made. Here the emitted fluorescence is predominantly spherically symmetric, without memory of the direction of the excitation illumination. The entire sphere centered at the fluorescent center must be used, and  $f_{fluor} = \frac{1}{2}(1 - \cos \theta)$ . We summarize these calculations in Table 6.

Table 6. Fractions of scattered and fluorescence illumination captured by the objective

Magnification M	N.A.	Angular aperture ( $2\theta$ )	$f_{scatt}$ (Worst case)	$f_{fluor}$
10X	0.3	$26.1^\circ$	0.0258	0.0129
40X	0.8	$74.0^\circ$	0.201	0.101
60X	1.0	$97.5^\circ$	0.341	0.171

Below in Table 7 we delineate the transmission factors for the BTS optical train, from laser line generator exit port to the line-scan camera sensor.

Table 7. Transmission factors for optical train

Optical element	Optical train transmission factors	
	Absorption imaging	Fluorescence imaging
Laser line generator exit port to rear face of diamond knife	0.5	0.5
Diamond knife collimator (overflow of minimum line width)	0.6	0.6

Development of the Brain Tissue Scanner  
Brain Networks Laboratory Technical Report

Quantum efficiency of fluor	N/A	0.3
Objective collection efficiency	0.026, 0.20, 0.34 (10X, 40X, 60X respectively)	0.013, 0.10, 0.17 (10X, 40X, 60X respectively)
Objective lens transmission	0.8	0.8
Filter cube transmission	1.0	0.8
Field lens transmission	0.8	0.8
Transfer lens transmission	0.8	0.8
Integrated transmission factor of optical train	0.0040, 0.031, 0.052 (10X, 40X, 60X respectively)	0.0005, 0.0037, 0.029 (10X, 40X, 60X respectively)

The objective-dependent illumination requirements at the source (Table 8) can now be calculated from the CW power requirements at the sensor (Table 5). The integrated transmission factors for absorptive and fluorescence scanning are tabulated in Table 7. The power requirements at the source depend on the objective and assume scanning at the maximum line rate supported by the camera.

Table 8. Illumination requirements at the source

Camera	Dalsa CT-F3-4096)	Dalsa CL-T5-2048 (color)		
		R	G	B
CW power at sensor ( $\mu$ W)	43.3	0.82	1.21	2.86
CW power at source (10X, absorptive) (mW)	11	0.21	0.30	0.72
CW power at source (40X, absorptive) (mW)	1.4	0.026	0.039	0.092
CW power at source (60X, absorptive) (mW)	0.8	0.015	0.023	0.055
CW power at source (10X, fluorescence) (mW)	87	1.6	2.4	5.7
CW power at source (40X, fluorescence) (mW)	12	0.22	0.33	0.77
CW power at source (60X, fluorescence) (mW)	1.5	0.03	0.04	0.1

#### Laser line generators: line width selection

A laser line generator is used to illuminate a strip of tissue parallel to the Y-axis, and hence perpendicular to the (X-axis) direction of the scan. In a TDI camera, all TDI registers must be simultaneously in focus, which accounts for the high sensitivity of the camera. Therefore the axis of the objective must be perpendicular to plane of the tissue being imaged. For knife-edge scanning the plane of tissue is essentially the top surface of the knife.

The laser line generator is used to illuminate a strip of tissue parallel to and just downstream from the knife edge. Ideally we center this illuminated line within 100 $\mu$ m of the knife edge, so as to minimize tissue distortion at the time of exposure of the illuminated strip. Calculations below are based on the Dalsa CT-F3-4096 camera (with 96 TDI registers). The other camera (Dalsa CL-T5) gives similar results. We tabulate below (Table 9) the width of the camera aperture (including all TDI registers) as back-projected to the object plane (the illuminated strip). For ease of comparison with other cameras, we also tabulate the results for 96 TDI registers.

Table 9. Illuminated line aperture at tissue surface

Objective Magnification M	Aperture back-projected from sensor (96 TDI)	TDI registers covered for 30 $\mu$ m line width
10X	2.5mm x 60 $\mu$ m	48
40X	0.625mm x 15 $\mu$ m	96
60X	0.417mm x 10 $\mu$ m	96

Overfilling the line aperture at the tissue surface wastes light; light outside the aperture is imaged outside the TDI registers and therefore not sensed. Under-filling the line aperture at the tissue surface means that outer TDI registers are not illuminated, and therefore a scanning mode with fewer TDI registers can be used. Defocusing the generated line to expand and fill the line aperture at the tissue surface accomplishes little; the TDI registers collect the same number of photons, albeit in more shift and accumulate actions.

#### **4.5 Microscope assembly**

##### Microscope objective focusing and retracting system

The system, based on precision linear bearings, allows the microscope objective lens to be retracted away from the specimen carrier for specimen change clearance. The original objective lens tube of the Nikon E600FN microscope will be used. A latch holds the objective in the retracting position. A micrometer screw on a sapphire plate provides focusing adjustment.

##### Two camera transfer lenses

These transfer lenses attach the camera (Dalsa CT-F3 or CL-T5) to the microscope port (OSI 38mm), positioning the camera at the proper optical distances from the field lens. The camera distance from the field lens is adjustable.

#### **4.6 Camera interface cards for image acquisition**

The image capture system uses three camera interface cards manufactured by Epix, Inc., Buffalo Grove, IL. The camera interface consists of two PIXCI D32A boards for the Dalsa CT-F3 monochrome line-scan camera and one PIXCI D2X board for the Dalsa CL-T5 color line-scan camera. These three boards, though initially mounted in a prototype provided server (Epix, Inc.), will be transferred to the master server (Dell 2550) of the five servers in the current configuration when Linux versions of the board drivers are available. (The five Dell servers are being converted to run under Linux.)

The Dalsa CT-F3-4096 camera requires two camera interface cards (PIXCI D32A). One board is required for two of the PCI buses in a dual-processor server. Pixels 1-2047 are sent to one board, pixels 2048-4095 are sent to the other, for a combined nominal data rate of 200MB/s. The Dalsa CL-T5-2048 color camera requires only one board (PIXCI D2X), again manufactured by Epix, Inc., receiving a nominal data rate of 75MB/s.

#### **4.7 Camera test configuration for the CT-F3 camera**

The camera test setup allows testing of the camera by itself before the rest of the system is operational. The Dalsa CT-F3 camera is provided a 5X macro lens (equivalent to a 2.5X microscope objective) with a field of view (FoV) of 10mm. The camera and its lens are then mounted directly to the granite bridge of the 3-axis stage at the proper position to obtain test images.

##### 50mm macro lens

Schneider Optics 50mm macro lens (Macro CPN-S 2.8/50 (mounted in reverse) 25-014796)  
Working Distance (lens front metal work to object) = 36 mm

##### Other Schneider Optics components

Macro to Leica Adapter 25-020054  
Unifoc 76 Focus Mount 21-013048  
M58 to M72 Adapter 21-013052  
9 M72 25mm Extension Tubes 21-026406  
M72 5mm Extension Tube 65-040621

M72 to Dalsa 3" Adapter 21-720030

## 5. Image Analysis and Data Storage System Specifications

### **5.1 Performance requirement: Real-time image data compression and 1TB dynamic data storage**

The *image analysis and data storage system* will enable data acquisition, data reduction (through filtering), 3D reconstruction, data storage and retrieval, and data visualization. Data generated by the scanner will normally be *filtered* to retain only the regions of interest (e.g., neuron cross-sections), approximately a 50:1 reduction for Golgi-like stained tissue. For the transgenic mouse brain we anticipate a worst-case data compression of 16:1 for GFP-stained tissue. Even after 16:1 data reduction, the *storage* requirements are still formidable: One 1cm<sup>3</sup> of tissue requires 32 terabytes/16, or approximately 2TB of storage. Only the initial data reduction, described above, will be attempted in real time. 3D reconstruction and visualization, as well as support for general data storage and retrieval, will be off-line while tissue is being scanned.

In common with rendering farms commonly used in the animation industry, we plan to use a multi-server configuration to perform initial data filtering in real time, storing this filtered data (the ROIs) initially in a distributed database housed in the servers. The key concept here is to maintain coarse-grained parallelism in the image analysis and data storage system. Scanning data from consecutive sweeps of a common vertical block of tissue, one scan-width wide, is sent to a common server. By this mechanism, data collected by the server can be filtered and compressed largely without reference to data in another server. Even neuron segments that cross the boundary between successive knife-edge sweeps can be independently processed, if redundantly, within the servers. All tissue is cut and indexed only once.

### **5.2 Image analysis and data storage system configuration**

The multi-server configuration is based on the Dell PowerEdge 2550 rack-mounted server, with options as enumerated below. Five servers are used in the initial configuration, with expansion to an 8-server configuration planned.

#### Multi-server storage system

Two initial servers (Dell PowerEdge 2550 or equivalent), to be expanded to 8 servers, configured as follows:

PowerEdge 2550 Intel Pentium III 1.0GHz w/256K CACHE

Second Processor: 1.0GHz w/256K CACHE

Incorporates the HE-SL chipset, which supports tri-peer PCI architecture for added I/O performance and increased bandwidth.

Chassis: rack-mounted, with room to accommodate three Epix camera interface cards/server

Power Supply: Redundant Power

Memory: 2GB SDRAM, 133 MHz, 4X512MB DIMMS

Primary Controller: None

5 Hard Drives: each 36GB, U160M, SCSI, 1 in., 10K HD

Hard Drive Configuration: Drives attached to embedded SCSI controller, No RAID

Additional Network Adapter: Intel Pro 1000 Gigabit Fiber Server Adapter (to servers only)

Operating System: Windows 2000 Server with 5 Client Licenses, 4 GB Utility partition

Tape Backup Unit: none

Tape Backup Software: none

Diskette Drive: 3.5 in., 1.44MB Floppy Drive

CDROM: 24X, IDE CD-ROM

Keyboard: Standard Windows Keyboard, Grey

Development of the Brain Tissue Scanner  
Brain Networks Laboratory Technical Report

Monitor: none

Mouse: Logitech System Mouse, Grey

Documentation: Electronic Documentation for PowerEdge 2550

Modem: none

Hardware Support Services: 3 Yrs. BRONZE, Next Business Day Onsite

Software Support Services: none

### Gigabit switching network

A gigabit network has been ordered to link together the multiple servers of the image analysis and data storage system. The Dell 2550 server comes equipped with an on-board gigabit network adapter. The network uses a Cisco switch described below. The servers are linked by short copper links; two of the servers have in, addition, Intel Pro 1000 gigabit fiber server adapters to link to a remote parallel computer.

The network configuration is described below:

1 Catalyst 3508G XL Enterprise Edition

1 24x7x4 Svc., WS-C3508G

10 1000BASE-SX 'Short Wavelength' GBIC (Multimode only)

## 6. Brain Tissue Scanning

### 6.1 Brain tissue scanning modes

High-resolution scanning (40X objective) is used for the 3D reconstruction of stained neurons and fibers in the brain tissue. Low-resolution scanning (10X objective) is used for cell counts and 3D reconstruction of somata.

Resolution in the Z-direction is determined by the thickness of the tissue sections, rather than by the optical resolution of the objective. Cubic voxels are attractive from a geometric modeling perspective. However, for high-resolution scanning, we have chosen the thicker 500nm section thickness, for increased signal strength, better tissue handling, and reduced cutting/scanning times. This decision will be reexamined after experimental data is available.

#### Monochrome high-resolution mode (neurons and fibers)

Sample at 250nm at 44kHz lines/s, each 4096 pixels wide (180MB/s). 40X objective. Usable knife width = 0.625mm. Thickness of ribbon = 500nm (1 x 1 x 2 voxels). ~Nyquist sampling:  $\frac{1}{2}$  RP = 0.256nm (green laser); effective pixels = 2440. Cutting speed = 44kHz x 250nm/sample = 11mm/s.

#### Color high-resolution mode (neurons and fibers)

Sample at 300nm at 10.7kHz lines/s, each 2048 pixels wide, 3 B/color (65.7MB/s). 40X objective. Usable knife width = 0.625mm. Thickness of ribbon = 500nm (1 x 1 x 2 voxels). Under-sampling:  $\frac{1}{2}$  RP = 0.256nm (green laser); effective pixels = 2048. Cutting speed = 10.7kHz x 300nm/sample = 3.21mm/s

#### Monochrome low-resolution mode (cell counts and somata morphology)

Sample at 600nm at 44kHz, each 4096 pixels wide (180MB/s). 10X objective. Usable knife width = 2.5mm. Thickness of ribbon = 600nm (cubic voxels). ~Nyquist-sampling:  $\frac{1}{2}$  RP = 0.683nm (green laser), effective pixels = 3660. Cutting speed = 44kHz x 600nm/sample = 26.4mm/s.

#### Color low-resolution mode (cell counts and somata morphology)

Sample at 1200nm at 10.7kHz, each 2048 pixels wide (65.7MB/s). 10X objective. Usable knife width = 2.5mm. Thickness of ribbon = 1200nm (cubic voxels). Under-sampling:  $\frac{1}{2}$  RP = 0.683nm (green laser), effective pixels = 2048. Cutting speed = 10.7kHz x 1200nm/sample = 12.8mm/s.

## 6.2 Data volumes for the rodent brain

Block dimensions (plastic-embedded brain)

Mouse: 13mm x 9.5mm x 6mm = 741 mm<sup>3</sup>

Rat: 22mm x 15mm x 10mm = 3,300 mm<sup>3</sup> (4.5 x mouse brain volume)

Data volumes/sweep (mouse brain, worst case)

Table 10. Data volumes/sweep (mouse brain, worst case)

Scan Mode	$\Delta X$ sampling interval (nm)	Scan width (pixels)	A-P length (pixels)	Bytes per voxel	Data volume (MB)
Monochrome high-resolution	250	4096 (2,500 effective)	52,000	1	213
Color high-resolution	300	2048	43,300	3	266
Monochrome low-resolution	600	4096 (3,660 effective)	21,700	1	88.9
Color low-resolution	1200	2048	10,800	3	66.4

Data volumes/sweep (rat brain, worst case)

Table 11. Data volumes/sweep (rat brain, worst case)

Scan Mode	$\Delta X$ sampling interval (nm)	Camera width (pixels)	A-P length (pixels)	Bytes per voxel	Data volume (MB)
Monochrome high-resolution	250	4096 (2500 effective)	88,000	1	360
Color high-resolution	300	2048	73,300	3	450
Monochrome low-resolution	600	4096	36,700	1	150
Color low-resolution	1,200	2048	18,300	3	112

Total data volumes (mouse brain, no compression)

Table 12. Total data volumes (mouse brain, no compression)

Scan Mode	Sampling intervals (nm) ( $\Delta X, \Delta Y, \Delta Z$ )	A-P length (pixels)	M-L width (pixels)	D-V height (pixels)	Bytes per voxel	Data volume (TB)
Monochrome high-resolution	250, 250, 500	52,000	38,000	12,000	1	23.7
Color high-resolution	300, 300, 500	43,300	31,700	12,000	3	49.4
Monochrome low-resolution	600, 600, 600	21,700	15,800	10,000	1	3.43
Color low-resolution	1,200, 1,200, 1,200	10,800	7,920	5,000	3	1.28

Total data volumes (rat brain, no compression)

Table 13. Total data volumes (rat brain, no compression)

Scan Mode	Sampling intervals (nm) ( $\Delta X$ , $\Delta Y$ , $\Delta Z$ )	A-P length (pixels)	M-L width (pixels)	D-V height (pixels)	Bytes per voxel	Data volume (TB)
Monochrome high-resolution	250, 250, 500	88,000	60,000	20,000	1	106
Color high-resolution	300, 300, 500	73,300	50,000	20,000	3	220
Monochrome low-resolution	600, 600, 600	36,700	25,000	16,700	1	15.3
Color low-resolution	1,200, 1,200, 1,200	18,300	12,500	8,300	3	5.70

### 6.3 Rodent brain scanning times

Given the total data volumes and data rates for the various scanning modes, we can easily compute the times to scan a rodent brain. Tables 13 and 14 below tabulate these results. These results are unburdened by the stage return overhead, which can run 30-50%. The unburdened scanning times for the rat run 4.47 times longer than for the mouse.

Furthermore observe that monochrome low-resolution scanning has been slowed down four-fold from the camera's maximum data acquisition rate. This choice accommodates the excessive source illumination CW power requirements of this mode, which can be traced back to the small entrance pupil to the 10X objective used in this scan mode. In practice we may be able to run the camera at nearer its maximum line sampling frequency.

Table 14. Mouse scanning times (unburdened by overhead)

Scan Mode	Sampling intervals (nm) ( $\Delta X$ , $\Delta Y$ , $\Delta Z$ )	Data volume (TB)	Data rate (MB/s)	Scan time (hr)
Monochrome high-resolution	250, 250, 500	23.7	180	36.6
Color high-resolution	300, 300, 500	49.4	65.7	209
Monochrome low-resolution	600, 600, 600	3.43	45*	21.2
Color low-resolution	1,200, 1,200, 1,200	1.28	65.7	5.41

Table 15. Rat scanning times (unburdened by overhead)

Scan Mode	Sampling intervals (nm) ( $\Delta X$ , $\Delta Y$ , $\Delta Z$ )	Data volume (TB)	Data rate (MB/s)	Scan time (hr)
Monochrome high-resolution	250, 250, 500	106	180	164

Development of the Brain Tissue Scanner  
Brain Networks Laboratory Technical Report

Color high-resolution	300, 300, 500	220	65.7	930
Monochrome low-resolution	600, 600, 600	15.3	45*	94.4
Color low-resolution	1,200, 1,200, 1,200	5.70	65.7	24.1

## 7. Acknowledgments

The work described above was supported by the following grant: *Development of Brain Tissue Scanner*, NSF-MRI Grant 0079874 (McCormick, Texas A&M, 9/1/00-8/31/01).

The original design submitted in the NSF-MRI proposal did not (1) envision the use of the diamond knife as an optical component of the system, nor (2) the use of water-immersion objectives for improved resolution, nor (3) allow for imaging of GFP green fluorescent protein and its other colored variants (XFP), nor (4) provide the image analysis and data storage system. These latter additions have entailed additional cost, which have been covered by the award by the Texas Engineering Experiment Station of PUF Equipment Funds (McCormick, November 15, 2000).

## 8. References

- [1] M. Born and E. Wolf, *Principles of Optics*, Fifth Edition, Pergamon Press, 1975, pp. 414, 429.
- [2] Ibid. Figs. 8.11, 8.12, p. 396.
- [3] Burton, B.P., *Automated 3D Reconstruction of Neuronal Structures from Serial Sections*, MS Thesis, Department of Computer Science, Texas A&M University, 1999.
- [4] Burton, B.P., B.H. McCormick, R. Torp, and J.H. Fallon, Three-dimensional reconstruction of neuronal forests, *Neurocomputing*, 38-40: 1643-1650, 2001.
- [5] Koh, W. and B.H. McCormick, Brain Microstructure database system: an exoskeleton to 3D reconstruction and modeling, *Neurocomputing*, 2002 (in press).
- [6] Koh, W. and B.H. McCormick, Organization and visualization of brain tissue volume data, *Neurocomputing*, 38-40: 1679-1685, 2001.
- [7] Koh, W. and B.H. McCormick, Distributed, web-based microstructure database for brain tissue, *Neurocomputing*, 32-33: 1065-1071, 2000.
- [8] McCormick, B. H., Brain tissue scanner enables brain microstructure surveys, *Neurocomputing*, 2002 (in press).
- [9] McCormick, B.H., Design of a brain tissue scanner, *Neurocomputing*, 26-27: 1025-1032, 1999.